Validating Identified Nonlinear Models With Chaotic Dynamics

L A Aguirre and S A Billings
Department of Automatic Control and Systems Engineering
University of Sheffield
P O Box 600
Mappin Street
Sheffield
S1 4DU

Research Report No 469

March 1993

VALIDATING IDENTIFIED NONLINEAR MODELS WITH CHAOTIC DYNAMICS

LUIS A. AGUIRRE and S. A. BILLINGS

Department of Automatic Control and Systems Engineering

University of Sheffield

PO. Box 600, Mappin Street — Sheffield S1 4DU - UK

e-mail:aguirre@acse.sheffield.ac.uk

Abstract

This paper investigates the effectiveness of several criteria for validating models which exhibit chaotic dynamics. Trajectories in the pseudo-phase-plane, Poincaré sections, bifurcation diagrams, the largest Lyapunov exponent and correlation dimension are considered. The Duffing-Ueda equation and four identified models are used as examples. The results show that models with similar invariants such as Poincaré sections, the largest Lyapunov exponent and correlation dimension may have very different bifurcation behaviors. This suggests that the requirement that an identified model should reproduce the bifurcation pattern of the original system is a very exacting criterion which is well suited for validation purposes.

1 Introduction

One of the great challenges in science is that of inferring qualitative and quantitative information from time series and this often involves determining a mathematical model of a system when the only information available is a set of measured data. This is the so-called *system identification problem* [Sõdeström and Stoica, 1989].

Irrespective of the approach used to solve the identification problem and regardless of the structure of the final model, the last step in any identification procedure should be the validation of the estimated model. The main objectives of validation are to seek answers to questions such as, is the identified model adequate, and under what conditions is the model adequate or representative of the system.

A trivial way of trying to answer such questions is to simulate both system and model under similar conditions and compare the respective responses. Besides being subjective,

this procedure lacks consistency when the model being validated is sensitive to initial conditions. Clearly, more sophisticated criteria are needed to accomplish this task.

The need for more general criteria has motivated researchers to investigate geometrical and statistical invariants which would provide a means of characterizing nonlinear systems possessing low-dimensional chaotic dynamics. Thus trajectories in the pseudo-phase-plane [Broomhead and King, 1986; Moon, 1987], Poincaré sections [Crutchfield and McNamara, 1987], bifurcation diagrams [Haynes and Billings, 1992], Lyapunov exponents [Wolf *et al.*, 1985; Abarbanel *et al.*, 1989, 1990] and the correlation dimension [Grassberger and Procaccia, 1983; Wolf and Bessoir, 1991] have been used to characterize and compare reconstructed attractors and identified models.

These criteria provide some answers to the questions posed above, but how effective are such criteria in validating mathematical models of chaotic systems? The main objective of this paper is totry to answer this question.

Several examples are provided which considerthe Duffing-Ueda equation and four different identified models. Although the main focus is on non-autonomous chaotic models it is believed that most of the results are also valid for autonomous chaotic and even non-chaotic nonlinear systems.

The next section provides a brief summary of the criteria under investigation. Section 3 presents the numerical results obtained for the models considered and the results are discussed in detail in Sec. 4. Finally, the main conclusions are reported in Sec. 5.

2 Brief Description of Some Criteria

2.1 Predictions

One of the most peculiar features of a chaotic system is the sensitive dependence on initial conditions. This makes nearby orbits diverge locally in state-space. Consequently, it is impossible to make accurate long-term predictions using a chaotic model.

The statistics which quantify the average local divergence of nearby trajectories along certain directions on the attractor are the Lyapunov exponents. It is known that the period during which accurate predictions can be made is proportional to the accuracy with

which the initial state was measured and inversely proportional to the largest Lyapunov exponent. In practice, no measurement can be performed with infinite accuracy and therefore no matter how good an identified model is, the predictions will eventually drift away from the original data. Indeed, if the identified model is to capture the qualitative behavior of the underlying system, these characteristics should be evident and if they are not the model is just a fit to one window of data and is not representative of the system. Consequently, the predictions will not be of much help in validating identified models if these are sensitive to initial conditions. In spite of this deficiency the use of predictions for chaotic model validation has been considered by some authors [Kargupta and Smith, 1991].

2.2 Correlation tests

Billings and Voon [1983; 1986] have introduced high-order correlation functions to detect the presence of unmodelled terms in the residuals of discrete models. Thus if a model of a system is adequate the following conditions should hold

$$\Phi_{\xi\xi}(\tau) = E[\xi(t-\tau)\xi(t)] = \delta(0) \tag{1.a}$$

$$\Phi_{u\xi}(\tau) = E[u(t-\tau)\xi(t)] = 0, \quad \forall\tau \tag{1.b}$$

$$\Phi_{u^{2\prime}\xi}(\tau) = E[(u^2(t-\tau) - \overline{u^2(t)})\xi(t)] = 0, \quad \forall\tau \tag{1.c}$$

$$\Phi_{u^{2\prime}\xi^2}(\tau) = E[(u^2(t-\tau) - \overline{u^2(t)})\xi^2(t)] = 0, \quad \forall\tau \tag{1.d}$$

$$\Phi_{\xi(\xi u)}(\tau) = E[\xi(t)\xi(t-1-\tau)u(t-1-\tau)] = 0, \quad \tau \geq 0 \tag{1.e}$$

where $\xi(t)$ are the residuals, defined as the difference between the actual measured output and the one-step-ahead predicted output, $u(t)$ is the input, the over-bar signifies mean value and $E[\cdot]$ denotes mathematical expectation.

These correlation functions were originally derived for non-autonomous models. In many practical situations however, no inputs are considered and the final models are obtained from time series instead of input-output pairs. In such cases the correlations functions which should be tested are different [Billings and Tao, 1991].

2.3 Pseudo-phase-space plots

One technique used in the analysis of nonlinear dynamical systems is to plot the steady-state trajectory of the system in the phase-space. For a system with one degree of freedom this can be achieved by plotting $\dot{y}(t)$ against $y(t)$. For low-order systems this procedure can be used to distinguish between different dynamical regimes.

In many practical situations only one variable is measured. In these cases an alternative procedure is to plot $y(t - T_p)$ against $y(t)$. These variables define the so-called pseudo-phase plane which is motivated by the fact that $y(t - T_p)$ is related to $\dot{y}(t)$. Consequently this plane should have properties similar to those of the phase plane [Moon, 1987].

A further advantage of this technique is that it enables the comparison of trajectories computed from continuous systems where $\dot{y}(t)$ is usually available, and from discrete models where $\dot{y}(t)$ is not often available and would have to be estimated.

The choice of T_p is not very critical and plotting a trajectory onto the pseudo-phase plane for varying values of T_p may give some insight regarding the information flow on the attractor [Fraser and Swinney, 1986].

Phase and pseudo-phase portraits have been used not only as a means of distinguishing different dynamical regimes, but also to demonstrate qualitative relationships between original and reconstructed attractors [Packard *et al.*, 1980; Broomhead and King, 1986; Adomaitis *et al.* 1991].

2.4 Poincaré sections

Consider a periodic orbit γ of some flow ϕ_t in $\mathbb{R}^n$ arising from a nonlinear vector field. Let $\Sigma \subset \mathbb{R}^n$ be a hypersurface of dimension $n-1$ which is transverse to the flow ϕ_t. Thus the first return or Poincaré map $P = \Sigma \rightarrow \Sigma$ is defined for a point $q \in \Sigma$ by

$$P(q) = \phi_\tau(q) \tag{2}$$

where τ is the time taken for the orbit $\phi_t(q)$ based at q to first return to Σ.

This map is very useful in the analysis of nonlinear systems since it takes place in a space which is of lower dimension than the actual system. It is therefore easy to see that

a fixed point of P corresponds to a periodic orbit of period $2\pi/\omega$ for the flow. Similarly, a subharmonic of period $k \times 2\pi/\omega$ will appear as k fixed points of P. Quasiperiodic and chaotic regimes can also be readily recognized using Poincaré maps. For instance, the first-return map of a chaotic solution is formed by a well-defined and finely-structured set of points for noise-free dissipative systems. Such maps have been used extensively in the validation of identified models and reconstructed attractors [Van Buskirk and Jeffries, 1985; Broomhead and King, 1986; Crutchfield and McNamara, 1987; Casdagli, 1989; Giona *et al.*, 1991; Gottwald *et al.*, 1992).

From the above definition it is clear that if a system has $n > 3$, the Poincaré map would require more than two dimensions for a graphical presentation. In order to restrict the plots to 2-dimensional figures, $y(t - T_p)$ is plotted against $y(t)$ at a constant period. For periodically driven systems the input period is a natural choice and the resulting plot is called a Poincaré section.

This procedure amounts to defining the Poincaré plane Σ_p in the pseudo-phase-space and then sampling the orbit represented in such a space. The choice of T_p is not critical but it should not be chosen to be too small nor too large compared to the correlation time of the trajectory. Otherwise the geometry and fine structure of the attractor would not be well represented.

Besides simplification in cases where $n > 3$, this procedure has two additional benefits, namely i) it allows Poincaré sections of models of different dimensions to be compared, and ii) similar sections can be obtained for continuous and discrete models. Thus comparison is again facilitated. The qualitative information conveyed by both Poincaré maps and sections are equivalent.

It is noted that if two Poincaré sections are to be compared, the Poincaré plane Σ_p should be the same for both sections. This could pose some problems in the case of discrete models since it is required that the models produce an output at the Poincaré sampling instants which may not agree with the model sampling rate. In the case of continuous systems which are integrated digitally this difficulty has been overcome [Hénon, 1982].

2.5 Bifurcation diagrams

Another useful tool for assessing the characteristics of the steady-state solutions of a system over a range of parameter values is the bifurcation diagram.

A point r of a bifurcation diagram of the kind considered in this work is defined as

$$r = \{ (y, A) \in \mathbb{R} \times I \mid y = y(t_i),\ A = A_0;\ t_i = K_{ss} \times 2\pi/\omega \} \tag{3}$$

where I is the interval $I = [A_i A_f] \subset \mathbb{R}$ and K_{ss} is a constant. This means that the point r is chosen by simulating the system for a sufficiently long time $K_{ss} \times 2\pi/\omega$ with $A = A_0$ to ensure that transients have died out before plotting $y(K_{ss} \times 2\pi/\omega)$ against A_0. In practice for each value of the parameter A, n_b points are taken at the instants

$$t_i = (K_{ss} + i) \times 2\pi/\omega \qquad i = 0, 1, ..., n_b - 1 \tag{4}$$

A bifurcation diagram will therefore reveal at which values of the parameter $A \in I$ the solution of the system bifurcates and how it bifurcates. When studying chaos such diagrams are also useful in detecting parameter ranges for which the system behavior is chaotic.

Similar diagrams as the one defined by Eqs. (3) and (4) have been suggested as a means of global analysis and *qualitative validation* of identified nonlinear models [Haynes and Billings, 1991]. In order to facilitate the comparison of similar bifurcation diagrams, the following quality index will be used

$$J_b = \sum_{i}^{N_b} (A_i - a_i)^2 w_i \tag{5}$$

where $A_i \in \mathbb{R}$ are the values of the parameter A for which the system bifurcates. The a_i's are defined likewise for the model being validated and $\mathbf{w} = [w_1\ w_2\ ...\ w_{N_b}]$ is a weighting vector. The summation is taken over all the (N_b) bifurcation points of interest.

Further details of bifurcations and Poincaré maps can be found in the literature [Guckenheimer and Holmes, 1983].

2.6 Lyapunov exponents

Lyapunov exponents measure the average divergence of nearby trajectories along certain directions in state space. A chaotic attracting set has at least one positive Lyapunov

exponent and no Lyapunov exponent of a non-chaotic attracting set can be positive. Consequently such exponents have been used as a criterion to determine if a given attracting set is or is not chaotic [Wolf, 1986].

The Lyapunov exponents of an attracting set of length N can be defined as [1]

$$\lambda_i = \lim_{N\to\infty} \frac{1}{N} \log_e j_i(N) \qquad i = 1, 2, ..., n \tag{6}$$

where the $\{j_i(N)\}_{i=1}^n$ are the absolute values of the eigenvalues of

$$[J(y_N)][J(y_{N-1})]...[J(y_1)] \tag{7}$$

where $J(y_i) \in \mathbb{R}^{n\times n}$ is the jacobian matrix of the n-dimensional differential equation (or discrete map) evaluated at y_i, and $\{y_k\}_{k=1}^N$ is a trajectory on the attractor. Note that n is the dynamical order of the system.

When reconstructing attractors from time series, it is common practice to embed the data in an m-dimensional state space where m is usually referred to as the embedding dimension. A famous theorem due to Takens [1980] (see also the paper by Packard *et al.* [1980]) states that if $m \geq 2n+1$ then the embedded attractor will retain metric properties of the original attractor, such as Lyapunov exponents, dimensions and entropies.

A similar situation occurs in system identification where usually the order of the identified model is also larger than n. Consequently the identified model will have more Lyapunov exponents than the original system. These 'extra' exponents are called *spurious Lyapunov exponents.*

The estimation of Lyapunov exponents is known to be a nontrivial task. The simplest algorithms [Wolf *et al.*, 1985; Moon, 1987] can only reliably estimate the largest Lyapunov exponent. Estimating the entire spectrum is a typically ill-conditioned problem and requires sophisticated algorithms [Wolf *et al.*, 1985; Parker and Chua, 1989]. Further problems arise when it comes to deciding which of the estimated exponents are *true* and which are *spurious* [Parlitz, 1992].

In view of such difficulties and the fact that the largest Lyapunov exponent, $\lambda_{largest}$, is in many cases the only positive exponent [2] and that this gives an indication of how

[1] Many authors use log_2 in this definition

[2] In this case the $\lambda_{largest} \geq h$, where h is the Kolmogorov-Sinai or metric entropy. Note that for dissipative systems (chaotic and non-chaotic) $\sum_{i=1}^n \lambda_i < 0$ [Eckmann and Ruelle, 1985; Wolf, 1986].

far into the future accurate predictions can be made, it seems appropriate to use $\lambda_{largest}$ to characterize a chaotic attracting set. Indeed, the largest Lyapunov exponent has been used in this way and to compare several identified models [Abarbanel *et al.*, 1989; 1990].

2.7 Correlation dimension

Another quantitative measure of an attracting set is the fractal dimension. In theory, the fractal dimension of a chaotic (non-chaotic) attracting set is non-integer (integer). Therefore, like the largest Lyapunov exponent, the fractal dimension can be used not only to diagnose chaos but also to provide some further dynamical information regarding the attracting set under consideration [Grassberger *et al.*, 1991].

The fractal dimension is related to the amount of information required to characterize a certain trajectory. If the fractal dimension of an attracting set is $D = d + \delta$, where $0 < \delta < 1$, then the smallest number of first-order differential equations required to describe the data is $d+1$.

There are several types of fractal dimension but for many strange attractors such measures give roughly the same value [Moon, 1987; Parker and Chua, 1989]. In this work the correlation dimension [3] [Grassberger and Procaccia, 1983] is used to compare the original attracting set to similar sets generated using the identified models.

A time series $\{y_i\}_{i=1}^{N}$ can be embedded in the phase space where it is represented as a sequence of m-dimensional points $\mathbf{y}_j = [y_j\ y_{j-1}\ \cdots\ y_{j-m+1}]$. Suppose the distance between two such points is [4] $S_{ij} = |\ \mathbf{y}_i - \mathbf{y}_j\ |$ then a correlation function is defined as [Grassberger and Procaccia, 1983]

$$C(\epsilon) = \lim_{N\to\infty} \frac{1}{N} (number\ of\ pairs\ (i,j)\ with\ S_{ij} < \epsilon) \tag{8}$$

The correlation dimension is then defined as

$$D_c = \lim_{\epsilon\to\infty} \frac{log_e\ C(\epsilon)}{log_e\ \epsilon} \tag{9}$$

[3] This measure can be seen as a *generalized dimension* and is considered to be the easiest to estimate reliably [Grassberger, 1986]

[4] Several norms can be used here, e.g. Euclidean, ℓ_1, etc.

For many attractors D_c will be (roughly) constant for values of ϵ within a certain range. The choice of m does influence the final value of D_c, thus in practice several estimates of the correlation dimension are obtained for increasing values of m. If the data were produced by a low-dimensional system, such estimates would converge after m has attained a critical value .

3 Validation Results

In this section the criteria described in Sec. 2 will be investigated in the context of model validation. This is the last step in any identification procedure and is of paramount importance since it is in this step that a model is declared valid or not.

In what follows, the well known Duffing-Ueda equation [Ueda, 1980]

$$\ddot{y} + k\dot{y} + y^3 = u(t) \tag{10}$$

with $k = 0.1$, was used to produce the original data by means of digital simulation. A fourth-order Runge-Kutta algorithm with an integration interval of $\pi/3000$ was used to simulate the response of the system to a specified input. Both, the input, $u(t)$, and the output, $y(t)$, were uniformly sampled at periods of $T = \pi/60$ s, this gives 120 points per orbit. These values have been chosen after a detailed study [Aguirre and Billings, 1993]. The resulting time sequences, with 1900 data points each, are shown in Fig. 1. These data were subsequently used to identify the following discrete polynomial models

Model **A**

$$\begin{aligned} y(t) &= 2.1261y(t-1) - 1.2579y(t-2) + 0.13155y(t-3) \\ &+ 0.15881 \times 10^{-3}y(t-3)^3 - 0.24897 \times 10^{-2}y(t-1)^3 \\ &+ 0.20041 \times 10^{-2}u(t-2) + 0.34772 \times 10^{-3}u(t-1) \end{aligned} \tag{11}$$

Model **B**

$$\begin{aligned} y(t) &= 2.1951y(t-1) - 1.5112y(t-2) + 0.44472y(t-3) \\ &- 0.13619y(t-4) + 0.73697 \times 10^{-2}y(t-6) + 0.35045 \times 10^{-3}u(t-1) \\ &- 0.23964 \times 10^{-2}y(t-1)^3 + 0.20541 \times 10^{-2}u(t-2) \end{aligned} \tag{12}$$

Model C

$$\begin{aligned} y(t) &= 2.1850y(t-1) - 1.3957y(t-2) + 0.23137y(t-3) \\ &- 0.20770 \times 10^{-1}y(t-4) + 0.33579 \times 10^{-3}u(t-1) \\ &- 0.33823 \times 10^{-2}y(t-1)^3 + 0.19267 \times 10^{-2}u(t-2) \\ &+ 0.11426 \times 10^{-2}y(t-1)^2y(t-2) \end{aligned} \tag{13}$$

Model D

$$\begin{aligned} y(t) &= 2.1579y(t-1) - 1.3203y(t-2) + 0.16239y(t-3) \\ &+ 0.22480 \times 10^{-3}y(t-3)^3 - 0.48196 \times 10^{-2}y(t-1)^3 \\ &+ 0.19463 \times 10^{-2}u(t-2) + 0.34160 \times 10^{-3}u(t-1) \\ &+ 0.35230 \times 10^{-2}y(t-1)^2y(t-2) \\ &- 0.12162 \times 10^{-2}y(t-1)y(t-2)y(t-3) \end{aligned} \tag{14}$$

The chief objective of this section is to compute the mathematical tools described in last section for the identified models and the original system, to see how they compare and to assess the real benefits of using these as practical criteria for model validation of real systems.

Predictions. As stated before, predictions are not very adequate for model validation specially if the models under consideration are chaotic. A typical scenario is shown in Fig. 2, where model **D** was used to predict the output of the system when excited by the input of Fig. 1. These time series were obtained by means of Runge-Kutta simulation for the continuous model and by recursive computation for the discrete model. Clearly, initial predictions are very accurate but they (unsurprisingly) diverge from the original time series for longer prediction times. This divergence is not necessarily due to inaccuracies in the model since it could be a consequence of the sensitive dependence on initial conditions.

Correlation tests. Figures 3a–d show the correlation functions for the identified models A–D, respectively. These were obtained using models **A–D**, a set of data similar to the one of Fig. 1 and Eqs. 1a–1e.

Trajectories. Figures 4a–d show the trajectories of the identified models **A–D** when they were driven by the input $u(t) = Acos(\omega t)$ with $A = 11$ and $\omega = 1$ rad/s. The

trajectory obtained from the original system is shown in Fig. 4e. Here $T_p = 4 \times \pi/60$ for models **A–D** and $T_p = 200 \times \pi/3000$ for the continuous system. These trajectories correspond to twenty five forcing periods.

Poincaré sections. Figures 5a–d show the Poincaré sections of models **A–D** for the same input as above and $T_p = 4 \times \pi/60$. The corresponding plot for the original system is displayed in Fig. 5e, where $T_p = 200 \times \pi/3000$. Figures 7a–c show the Poincaré sections of models **C**, **D** and Eq. (10) for $u(t) = 5.75cos(t)$. These figures have 10000 points each.

Bifurcation diagrams. The bifurcation diagrams of the identified models are depicted in Figs. 6a–d. The varying parameter, sometimes called the control parameter, was the amplitude of the sinusoidal input which was varied in the range $4.5 \leq A \leq 12$. 750 equidistant values within this range were taken with $K_{ss} = 400$ and $n_b = 20$. The bifurcation diagram of the original system is shown in Fig. 6e. The quality index defined in Eq. (5) has been calculated for models **C** and **D** only because models **A** and **B** do not have all of the bifurcation points of the original system. The computed values are shown in Table 1.

Largest Lyapunov exponent. The Largest Lyapunov exponents were calculated using the standard algorithm, see for instance Moon [1987], with a time series corresponding to 7500 forcing periods ($N = 7500 \times 120 = 9 \times 10^5$) and a Lyapunov interval of 30. The value of $\lambda_{largest}$ estimated for the system is in excellent agreement with those obtained by Moon [1987] and Ueda [1979]. The estimated values of $\lambda_{largest}$ are shown in Table 1 for two different attractors (at A=5.75 and A=11).

It is noted that in all the cases investigated, the mathematical models were available and consequently the jacobian matrices were derived analytically. This greatly facilitated the computation of the Lyapunov exponents.

Correlation dimension. The correlation dimension has been estimated using data series of 10000 points. The distances S_{ij} were computed using 200 randomly chosen points (in state-space) which were uncorrelated with the data, see Packard and Chua [1989] for details. The embedding dimension was varied in the range $3 \leq m \leq 7$. For all models D_c had converged for $m = 7$. The estimated values of D_c with $m = 7$ for the two attractors aforementioned are provided in Table 1.

The Lyapunov dimension, D_{KY}, of the original system obtained via the Kaplan-Yorke conjecture [Kaplan and Yorke, 1979] for the attractors at A=5.75 and A=11 was 2.53 and

2.50, respectively. These results seem consistent since it is known that D_{KY} is an upper bound for the correlation dimension [Grassberger and Procaccia, 1983].

Table 1. $\lambda_{largest}$, D_c and J_b for the models considered

	A=11		A=5.75		
Model	$\lambda_{largest}$	D_c	$\lambda_{largest}$	D_c	J_b
Orig.	0.111	2.19 ± 0.02	0.099	2.10 ± 0.05	0.000
A	0.102	2.26 ± 0.04	—	—	—
B	0.109	2.19 ± 0.04	—	—	—
C	0.114	2.46 ± 0.06	0.049	1.80 ± 0.02	0.295
D	0.115	2.34 ± 0.05	0.093	2.05 ± 0.04	0.012

4 Discussion

The main difficulty in using predictions in model validation is that there seems to be no way to distinguish between discrepancies due to model inaccuracies and those due to sensitive dependence on initial conditions. It is noted that even short-term predictions are hampered if the data are noisy no matter how good the model is.

On the other hand, if the data are very clean the predictions could only usefully give a first impression of the behavior of the models being validated. This information, however, is very rough and rather abstract and would be of little help in validating models with no *evident* problems.

The correlation tests indicate the need for extra terms in the model. In cases where noise-free data are used, correlation in the residuals may be dominated by numerical errors such as roundoff errors. This calls for caution when interpreting such results.

The correlation functions of models **A** and **B** suggest that they are biased. On the other hand, the correlation plots of models **C** and **D** are quite acceptable. In a real situation, due to some amount of noise in the data, all of the correlation functions for the latter would certainly fall into the 95% confidence bands.

The correlation functions were not devised as *quality indices* and therefore it would be impossible to choose between models C and D based on these functions alone.

The trajectories in Figs. 4a–d should be compared to the one obtained from the original system and shown in Fig. 4e. Clearly, the overall shape and the location of the attractor in the pseudo- phase plane are very similar in all cases. This limits the usefulness of this technique in model validation. The main difference among the plots is the density of trajectories in some regions of the plane. This information, interesting as it might be, is not very useful since it is rather subjective. Further, these figures were obtained by plotting the trajectories over a few (twenty five) forcing periods only. Thus a region which was less visited during the period considered, could have had many more trajectories crossing into it if a longer simulation had been performed.

The Poincaré sections displayed in Figs. 5a–e were obtained after simulation over ten thousand input periods. This ensures that a region which was not visited would be very unlikely to be visited if the system had been simulated for a longer time. As can be seen, all the sections are very similar. It is noted that the use of Poincaré sections seems to be a very popular criterion for comparing models despite the limitations which are shown here [Van Buskirk and Jeffries, 1985; Broomhead and King, 1986; Crutchfield and McNamara, 1987; Casdagli, 1989; Giona *et al.*, 1991; Gottwald *et al.*, 1992].

The bifurcation diagram for the system of Eq. (10) is shown in Fig. 6e. This diagram gives a precise indication of how the system bifurcates as the input amplitude is varied. Beginning at $A \approx 4.86$ the system undergoes a period doubling (flip) bifurcation. This happens again at $A \approx 5.41$ and characterizes the well known period doubling route to chaos [Feigenbaum, 1983]. Another similar cascade begins at $A \approx 9.67$ preceding a different chaotic regime. Two chaotic windows can be distinguished at approximately $5.55 \leq A \leq 5.82$ and $9.94 \leq A \leq 11.64$. At $A \approx 6.61$ the system undergoes a supercritical pitchfork bifurcation and at $A \approx 9.67$ it undergoes a subcritical pitchfork bifurcation. The bifurcation diagram begins and ends with period-1 regimes and displays period-3 dynamics for $5.82 \leq A \leq 9.67$.

A rapid view of the bifurcation diagrams reveals that the dynamical bifurcation pattern of model D is the closest to the original system. Models A and B lack the pitchfork bifurcations, the first chaotic window and display extra chaotic regimes which are not

present in the original system.

On the other hand, models C and D have all the bifurcations in the considered range of parameter values. However, some deficiencies can be pointed out in the diagram of model C, namely the displacement of the pitchfork bifurcations and the width of the low-amplitude chaotic window (a detailed bifurcation diagram showed that model C is chaotic in the range $5.74 \leq A \leq 5.82$). These differences can be quantified using the bifurcation quality index defined in Eq. (5) where $\{w_i\}_{i=1}^{9} = 1$ was chosen. The calculated index is shown in Table 1 together with the largest Lyapunov exponent and the correlation dimension.

In the examples above, the invariants of the original system were obtained directly from the model, Eq. (10). However, in a real application the model of the system would obviously not be known *a priori* and therefore it is natural to enquire if the use of the criteria investigated in this paper would be viable since the invariants would have to be obtained directly from the system.

The correlation functions [Billings and Voon, 1983; 1986] can be easily obtained from the identified model. It is known, however, that it is very difficult and sometimes impossible to measure long stationary time series from certain systems [Grassberger *et al.*, 1991] and thus stationarity may only be guaranteed over short periods of time in a real experiment. Because the reliable calculation of Lyapunov exponents and fractal dimensions usually requires long stationary data series the use of such statistics in model validation could be difficult to implement in practice.

Regarding the significance of using Lyapunov exponents in the context of model validation, it has been noted that "calculations of orbital divergence rates necessarily characterize the properties of the given data set, and not necessarily the underlying dynamical system... in general it is not possible to independently confirm exponents determined from experimental data" [Wolf, 1986 p. 280]. Further, in the case of noisy data, it has been argued that the Lyapunov exponents are *not* rigorously defined [Wolf, 1986].

For a good account regarding the difficulties of estimating Lyapunov exponents and fractal dimensions from real data, see the paper by Wolf and Bessoir [1991]. Grassberger *et al.* [1991] also discuss similar issues concerning the estimation of the correlation dimension from real time series.

By contrast, pseudo-phase plots, Poincaré sections and bifurcation diagrams have been satisfactorily obtained directly from the original system in a number of practical situations [Arecchi and Califano, 1984; Vallée *et al.*, 1984; Van Buskirk and Jeffries, 1985; Moon, 1987; Molteno and Tufillaro, 1990; Murali and Lakshmanan, 1991; Gottwald *et al.*, 1992] and appear to be better suited for model validation. Casdagli [1989] has suggested a procedure to identify Poincaré sections and bifurcation diagrams from data obtained from the original system.

During the course of the present investigation, about one hundred models have been considered. Very few models presented a complete bifurcation diagram (as those of models **C** and **D**). However, most of the models had Poincaré sections similar to the original one, see Fig. 5e. Thus to identify models which reproduce the original bifurcation pattern has proved to be far more difficult than to obtain models with acceptable Poincaré sections. This is a consequence of the bifurcation diagram being a *global* invariant in the sense that it is valid over a *range* of parameter values. By contrast, the Poincaré sections and all other criteria considered in this paper are *local* invariants of the data which is usually obtained from the system operating at a *single* point in the parameter space. This *global* property can be further verified by noting that for A=5.75 the invariants of model **D** (see Poincaré sections of Figs. 7a–c and Table 1, it is noted that models **A** and **B** present regular motion for this input) are still close to those of the original model whereas the invariants of models **A**, **B** and **C** clearly reveal that they are inadequate for such a range of values of A.

It is worth emphasising however that when validating a model it is very important to consider the final application which is intended. In certain applications a model might be required which is accurate over a narrow range of parameter values and therefore *local invariants* may prove more helpful in such situations. But since the range of parameter values over which a model is required to be accurate can be easily taken into account by choosing different weights in Eq. (5), the bifurcation diagrams in conjunction with the respective quality indices still seem more appropriate for validation purposes.

Finally, it is noted that the bifurcation diagrams appear to be more sensitive to parameter variations than Poincaré sections. Investigating the Duffing-Holmes equation, Holmes and Rand [1976 p. 252] have noted: "... an arbitrarily small perturbation of

Duffing's equation in the space of all three or four parameter families could destroy the qualitative nature of the bifurcation set".

5 Conclusions

The validation of nonlinear models which possess chaotic dynamics has been studied in detail by comparying the properties of several identified models with a bench test example based on the Duffing-Ueda equation. The following criteria have been investigated: i) predictions, ii) correlation tests, iii) pseudo-phase plots, iv) Poincaré sections, v) bifurcation diagrams, vi) largest Lyapunov exponent and vii) correlation dimension. The central objective has been to assess the real benefit of using such criteria as measures of the quality of the identified model. One of the main results that has been reported is that models with considerably different bifurcation behavior may exhibit similar Poincaré sections within chaotic windows. This is an important result because Poincaré sections have been widely used in model validation problems. Although the focus of the current study was chaotic models, most of the reported results are also valid for regular nonlinear systems.

Acknowledgements LAA gratefully acknowledges financial support from the Brazilian Council of Scientific and Technological Development - CNPq, under grant 200597/90-6. SAB gratefully acknowledges that this work was supported by SERC under grant GR/H 35286

References

ABARBANEL, H.D.I., BROWN, R. AND KADTKE, J.B. [1989] "Prediction and system identification in chaotic nonlinear systems: time series with broadband spectra," *Phys. Lett* **138**(8), 401–408.

ABARBANEL, H.D.I., BROWN, R. AND KADTKE, J.B. [1990] "Prediction in chaotic nonlinear systems: Methods for time series with broadband Fourier spectra," *Phys. Rev. A* **41**(4), 1782–1807.

ADOMAITIS, R.A., FARBER, R.M., HUDSON, J.L., KEVREKIDIS, I.G., KUBE, M. AND LEPEDES, A.S. [1990] "Application of neural nets to system identification and bifurcation analysis of real world experimental data," in *Neural Networks: Biological computers or electronic brains*, Springer Verlag, Paris, 87–97.

AGUIRRE, L.A. AND BILLINGS, S.A. [1993] "Digital simulation and discrete modelling of a chaotic system," (submitted for publication).

ARECCHI, F.T. AND CALIFANO, A. [1984] "Low-frequency hopping phenomena in a nonlinear system with many attractors," *Phys. Lett.* **101A**(9), 443–446.

BILLINGS, S.A. AND VOON, W.S.F. [1983] "Structure detection and model validity tests in the identification of nonlinear systems," *IEE Proceedings Pt. D* **130**(4), 193–199.

BILLINGS, S.A. AND VOON, W.S.F. [1986] "Correlation based model validity tests for non-linear models," *Int. J. Control* **44**(1), 235–244.

BILLINGS, S.A. AND TAO, Q.H. [1991] "Model validation tests for nonlinear signal processing applications," *Int. J. Control* **54**, 157–194.

BROOMHEAD, D.S. AND KING, G.P. [1986] "Extracting qualitative dynamics from experimental data," *Physica D* **20**, 217–236.

CASDAGLI, M. [1989] "Nonlinear prediction of chaotic time series," *Physica D* **35**, 335–356.

CRUTCHFIELD, J.P AND MCNAMARA, B.S. [1987] "Equations of motion from a data series," *Complex Systems* **1**, 417–452.

ECKMANN, J.P. AND RUELLE, D. [1985] "Ergodic theory of chaos and strange attractors," *Rev. Mod. Phys.* **57**(3), 617–656.

FEIGENBAUM, M.J. [1983] "Universal behaviour in nonlinear systems," *Physica D* **7**, 16–39.

FRASER, A.M. AND SWINNEY, H.L. [1986] "Independent coordinates for strange attractors from mutual information," *Phys. Rev. A* **33**(2), 1134–1140.

GIONA, M., LENTINI, F. AND CIMAGALLI, V. [1991] "Functional reconstruction and local prediction of chaotic time series," *Phy. Rev. A* **44**(6), 3496–3502.

GOTTWALD, J.A., VIRGIN, L.N. AND DOWELL, E.H. [1992] "Experimental mimicry of Duffing's equation," *J. Sound and Vibration* **158**(3), 447–467.

GRASSBERGER, P. AND PROCACCIA, I. [1983] "Measuring the strangeness of strange attractors," *Physica D* **9**, 189–208.

GRASSBERGER, P. [1986] "Estimating the fractal dimensions and entropies of strange attractors," in *Chaos*, ed. Holden A.V., Manchester University Press, 291–311.

GRASSBERGER, P., SCHREIBER, J. AND SCHAFFRATH, C. [1991] "Nonlinear time sequence analysis," *Int. J. Bifurcation and Chaos* **1**(3), 521–547.

GUCKENHEIMER, J. AND HOLMES P. [1983] *Nonlinear oscillations, dynamical systems, and bifurcation of vector fields*, Springer-Verlag, New York.

HAYNES, B.R. AND BILLINGS, S.A. [1991] "Global analysis and model validation in nonlinear system identification," *J. of Nonlinear Dynamics* (to appear)

HÉNON, M. [1982] "On the numerical computation of Poincaré maps," *Physica D* **5**, 412–414.

HOLMES, P.J. AND RAND, D.A. [1976] "The bifurcations of Duffing's equation: an application of catastrophe theory," *J. Sound and Vibration* **44**(2), 237–253.

KAPLAN, J.L. AND YORKE, J.A. [1979] "Chaotic behavior of multidimensional difference equations," in *Functional differential equations and approximation of fixed points*, eds. Peitgen H.O. and Walter H.O., Lecture Notes in Mathematics, vol 730, Springer Verlag, 204–227.

KARGUPTA, H. AND SMITH, R.E. [1991] "Ssystem identification with evolving polynomial networks," *Proc. of the 4th Int. Conf. of Genetic Algorithms*, ed.Belew R., Morgan Kaufmann Publrs., 370–376.

MOLTENO, T.C.A. AND TUFILLARO, N.B. [1990] "Torus doubling and chaotic string vibrations: experimental results," *J. Sound and Vibration* **137**(2), 327–330.

MOON, F.C. [1987] *Chaotic Vibrations - an introduction for applied scientists and engineers*, John Willey and Sons.

MURALI, K. AND LAKSHMANAN, M. [1991] "Bifurcation and chaos of the sinusoidally-driven Chua's circuit," *Int. J. Bifurcation and Chaos* **1**(2), 369–384.

PACKARD, N.H., CRUTCHFILED, J.P., FARMER, J.D. AND SHAW, R.S. [1980] "Geometry from a time series," *Phys. Rev. Lett.* **45**(9), 712–716

PARKER, T.S. AND CHUA, L.O. [1989] *Practical numerical algorithms for chaotic systems*, Springer Verlag.

PARLITZ, U. [1992] "Identification of true and spurious Lyapunov exponents from time series," *Int. J. Bifurcation and Chaos* **2**(1), 155–165.

SÖDERSTRÖM, T. AND STOICA, P. [1989]. *System Identification*, Prentice Hall.

TAKENS, F. [1980] "Detecting strange attractors in turbulence," in *Dynamical systems and turbulence*, eds. Rand D.A. and Young L.S., Lecture Notes in Mathematics, vol. 898, Springer Verlag, Berlin, 366–381.

UEDA, Y. [1979] "Randomly transitional phenomena in the system governed by Duffing's equation," *J. Stat. Phys.* **20**, 181–196.

UEDA, Y. [1980] "Steady motions exhibited by Duffing's equation: A picture book of regular and chaotic motions," in *New approaches to nonlinear problems in dynamics*, ed. Holmes P.J., SIAM, 311–322.

VALLÉE, R., DELISLE, C. AND CHROSTOWSKI, J. [1984] "Noise versus chaos in acousto-optic bistability," *Phys. Rev. A* **30**(1), 336–342.

VAN BUSKIRK, R. AND JEFFRIES, C. [1985] "Observation of chaotic dynamics of coupled nonlinear oscillators," *Phys. Rev. A* **31**(5), 3332–3357.

WOLF, A., SWIFT, J.B., SWINNEY, H.L. AND VASTANO, J.A. [1985] "Determining Lyapunov exponents from a time series," *Physica D* **16**, 285–317.

WOLF, A. [1986] "Quantifying chaos with Lyapunov exponents," in *Chaos*, ed. Holden A.V., Manchester University Press, 273–290

WOLF, A. AND BESSOIR, T. [1991] "Diagnosing chaos in the Space Circle," *Physica D* **50**, 239-258.

Captions

Fig. 1. Typical input and output data used in the identification

Fig. 2. (- -) Measured output, and (—) typical predicted output for a chaotic model

Fig. 3. Correlation functions for models (a) **A**, (b) **B**, (c) **C** and (d) **D**

Fig. 4. Trajectories in the pseudo-phase plane for models (a) **A**, (b) **B**, (c) **C**, (d) **D** and (e) Eq. (10)

Fig. 5. Poincaré sections for the input $u = 11cos(t)$ for models (a) **A**, (b) **B**, (c) **C**, (d) **D** and (e) Eq. (10)

Fig. 6. Bifurcation diagrams for models (a) **A**, (b) **B**, (c) **C**, (d) **D** and (e) Eq. (10)

Fig. 7. Poincaré sections for the input $u = 5.75cos(t)$ for models (a) **C**, (b) **D** and (c) Eq. (10)

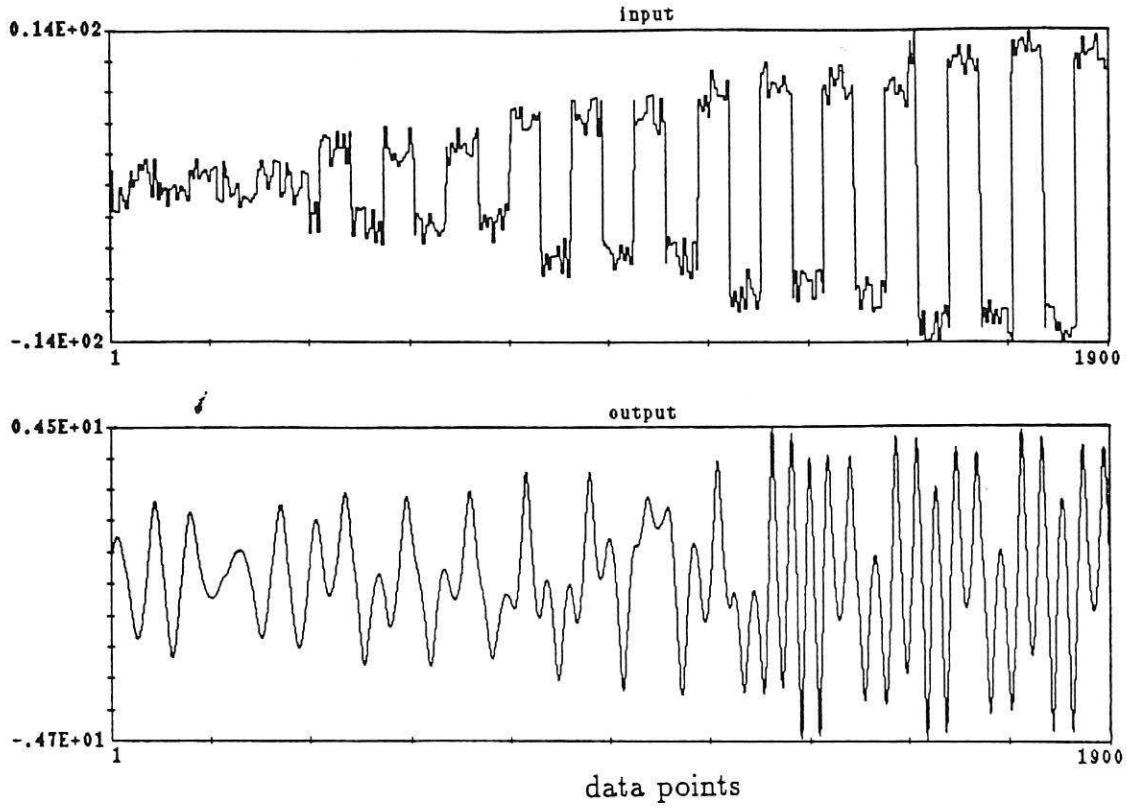

FIGURE 1

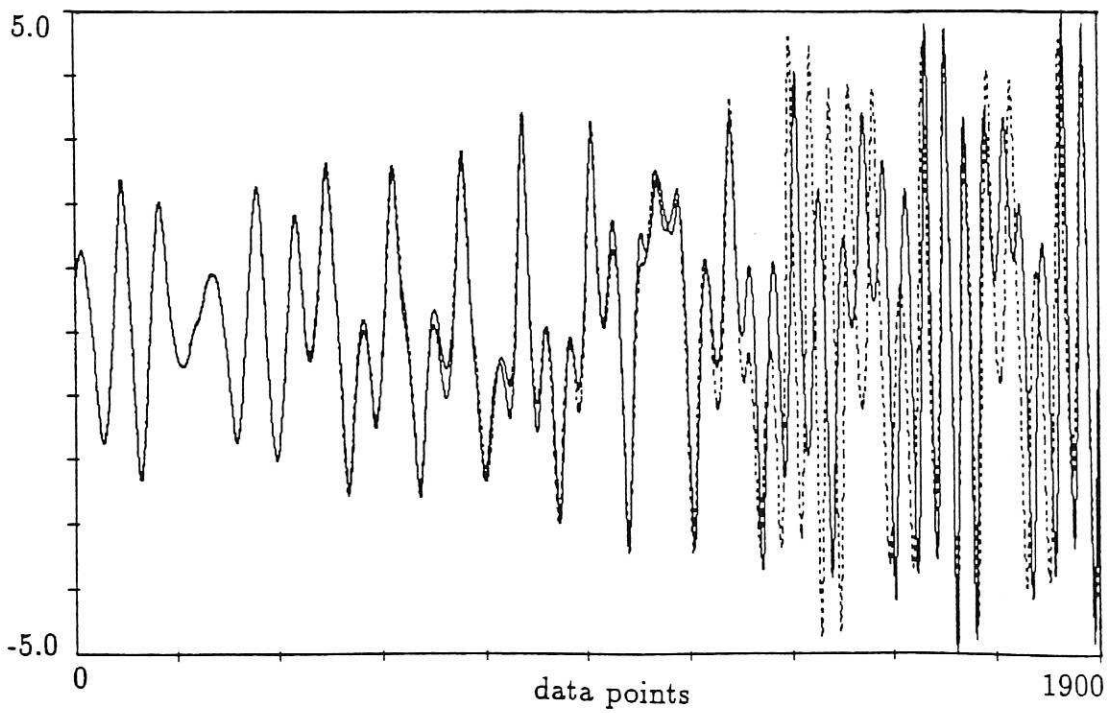

FIGURE 2

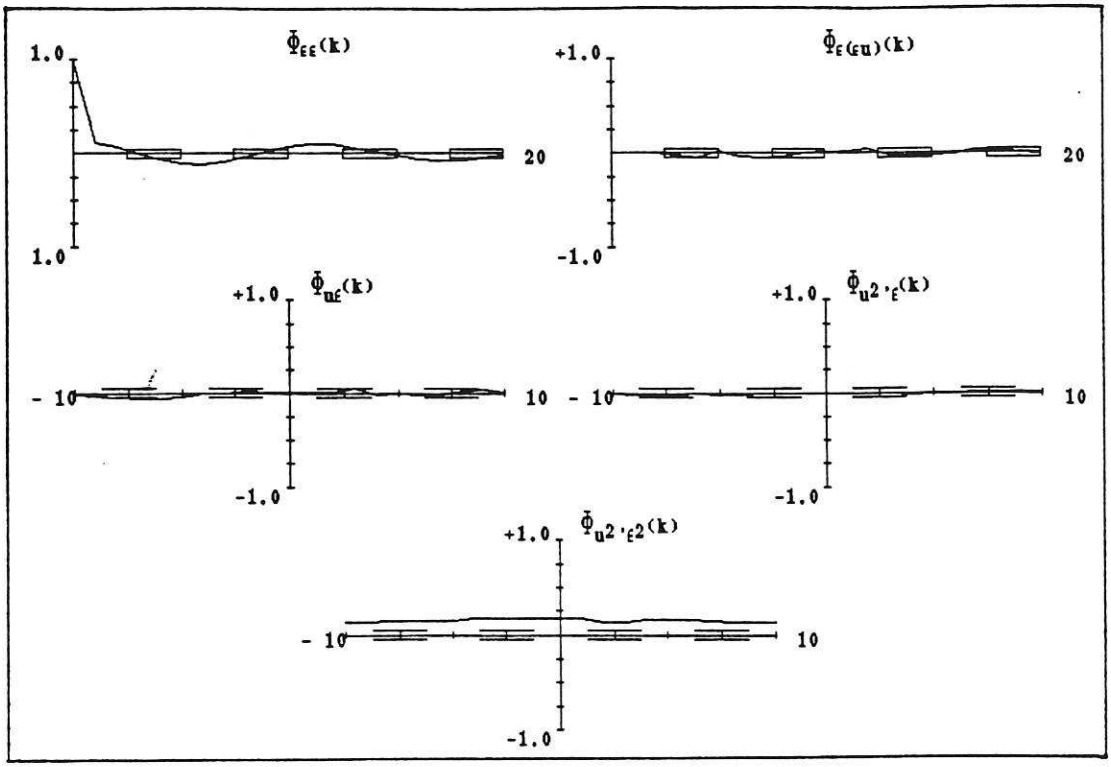

FIGURE 3a

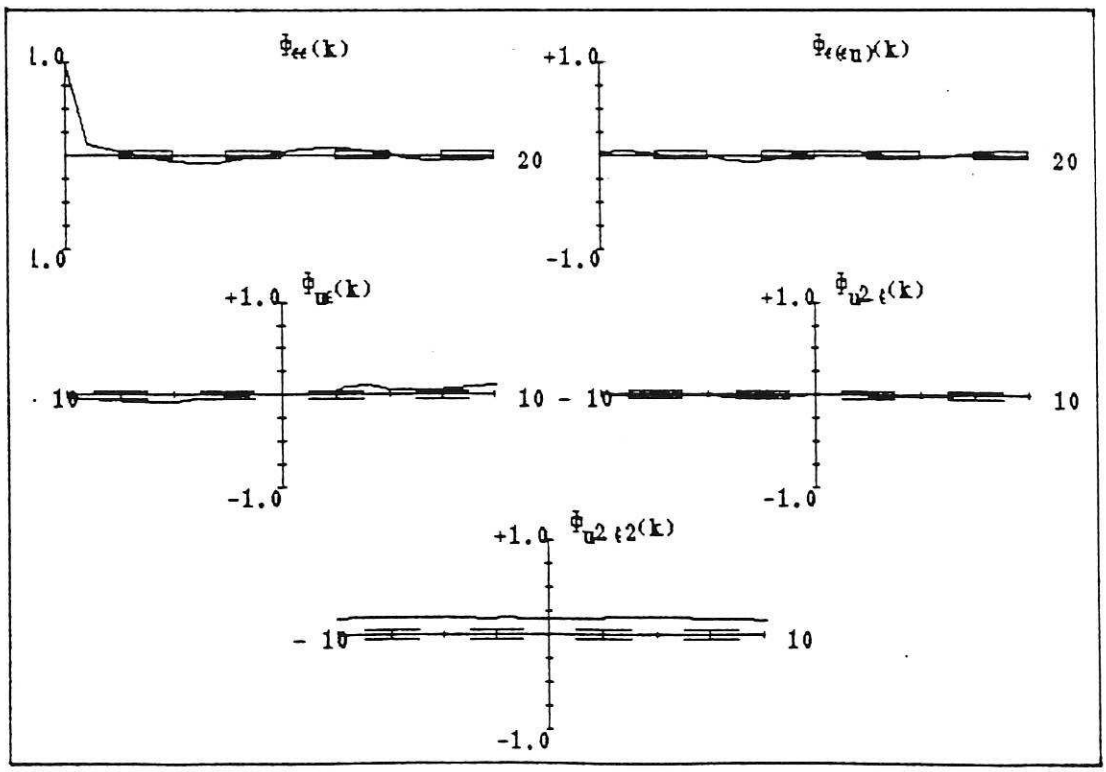

Figure 3b

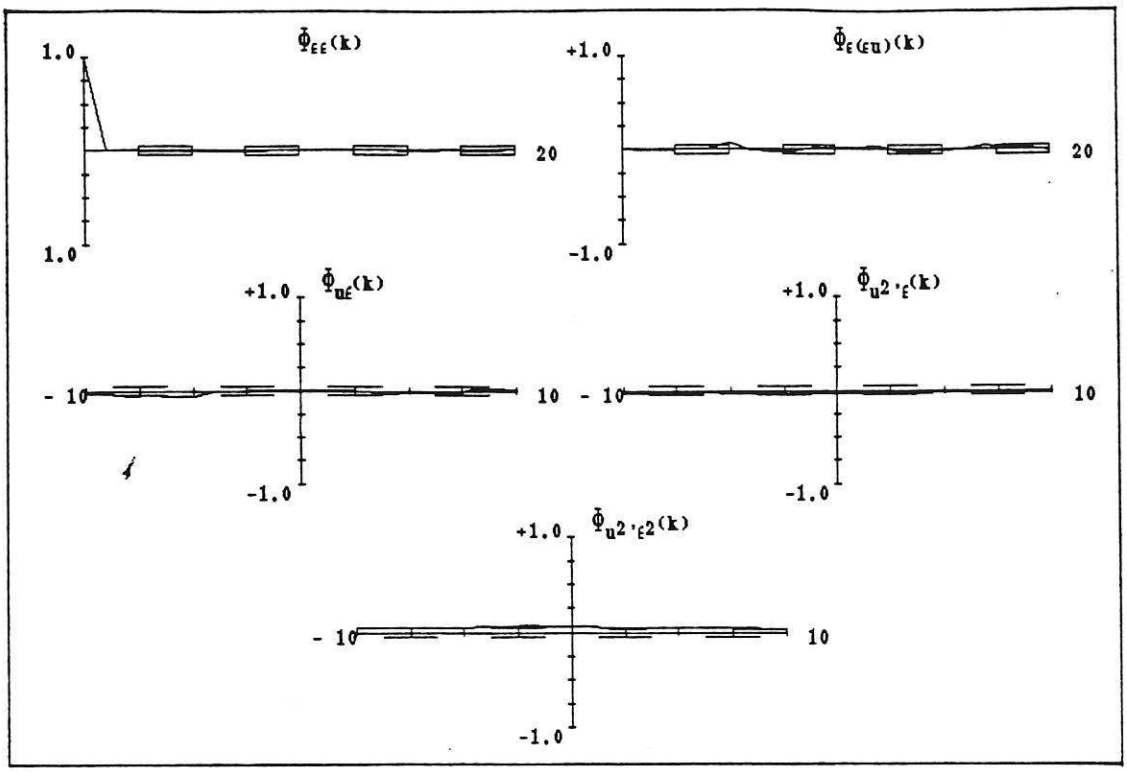

FIGURE 3c

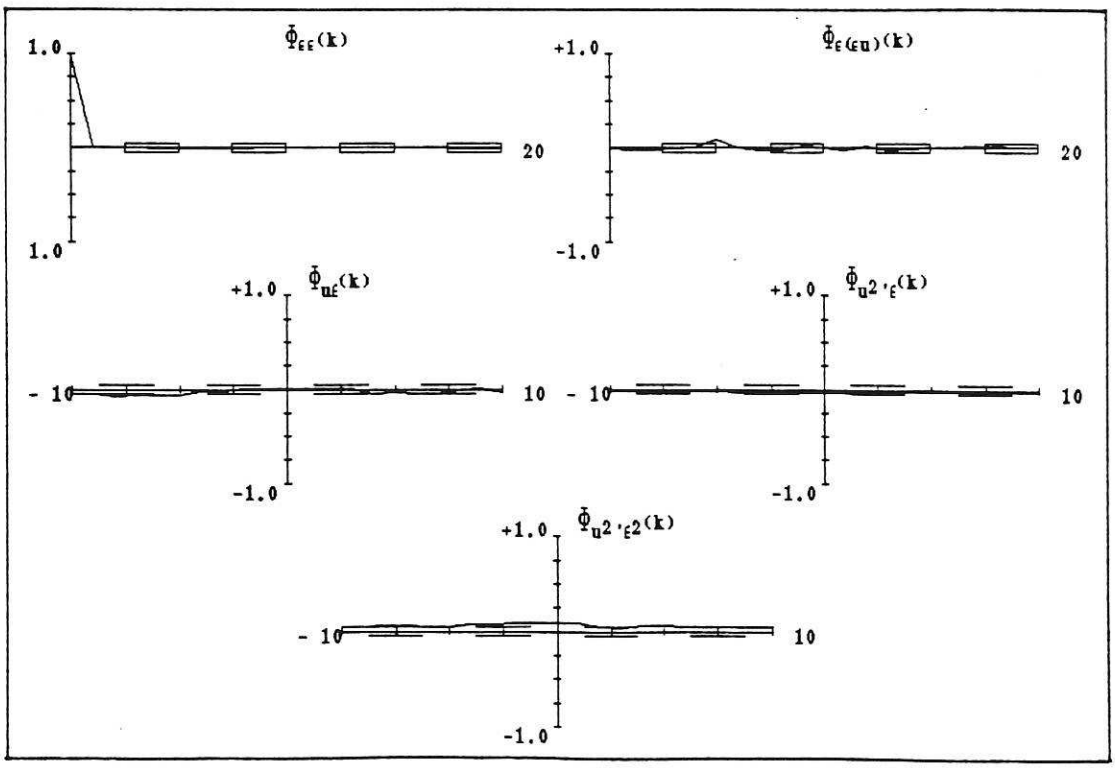

FIGURE 3d

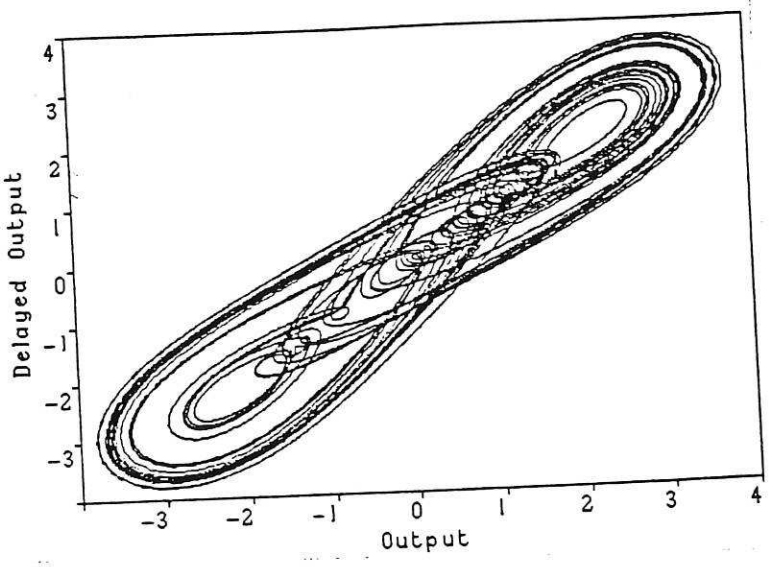

FIGURE 4a

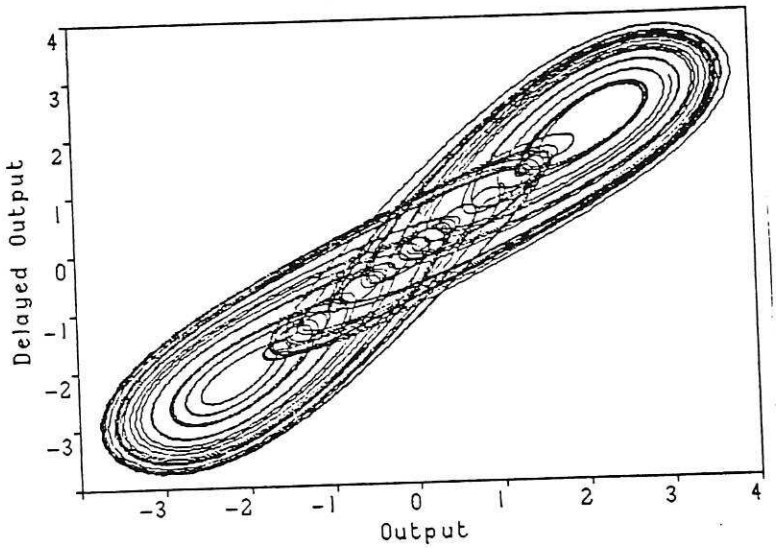

FIGURE 4b

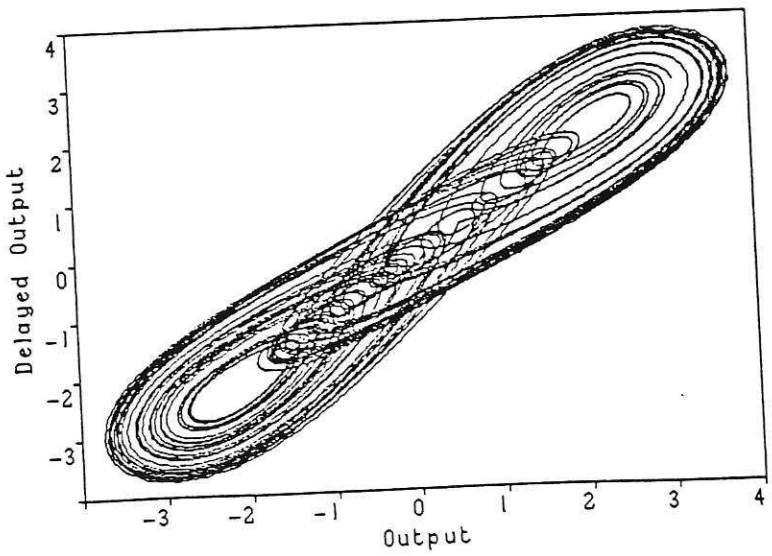

FIGURE 4c

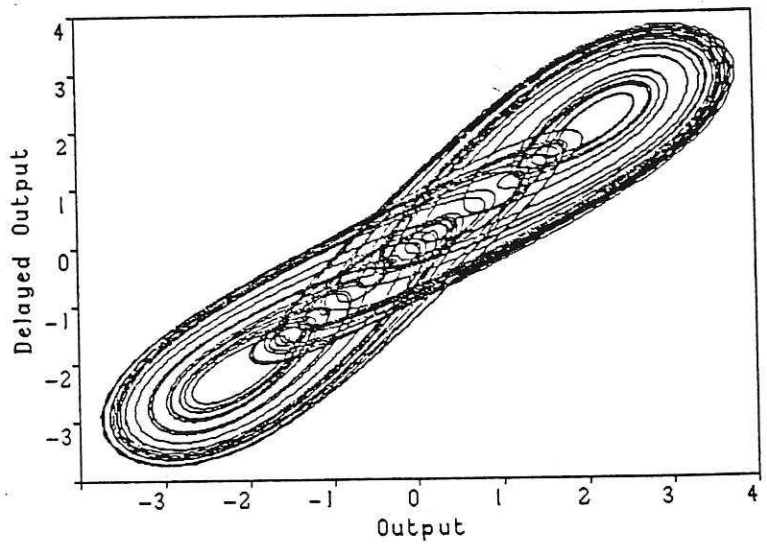

FIGURE 4d

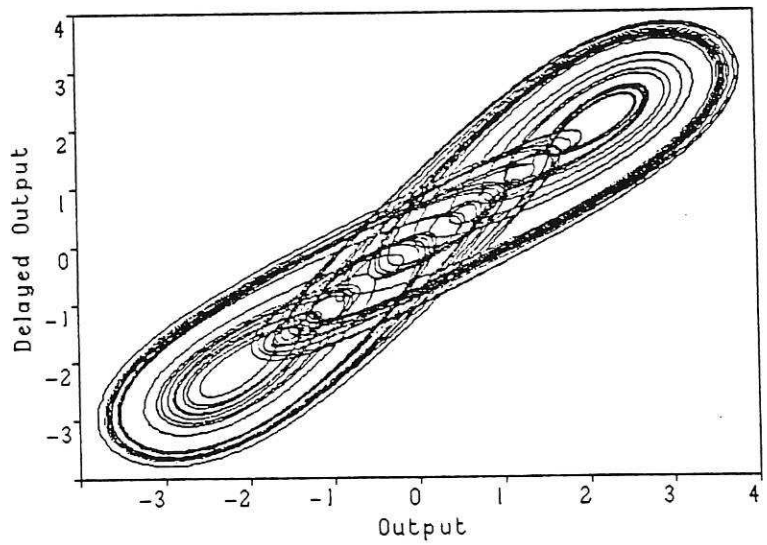

FIGURE 4e

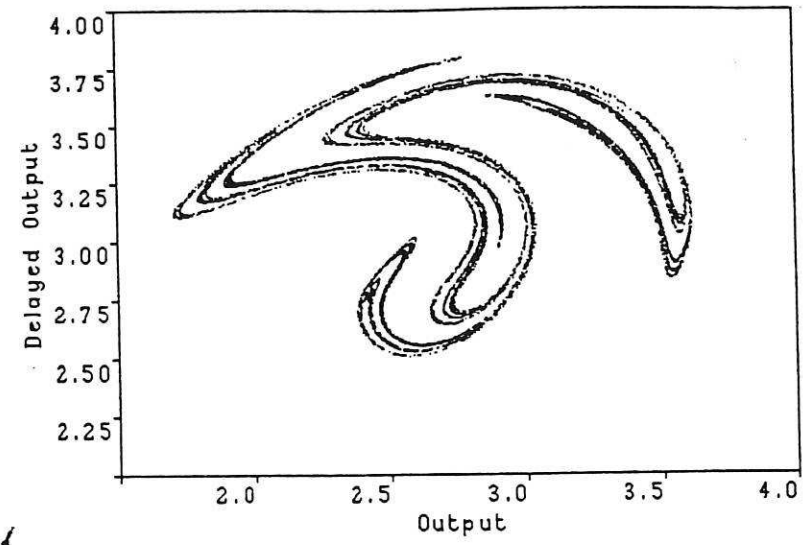

FIGURE 5a

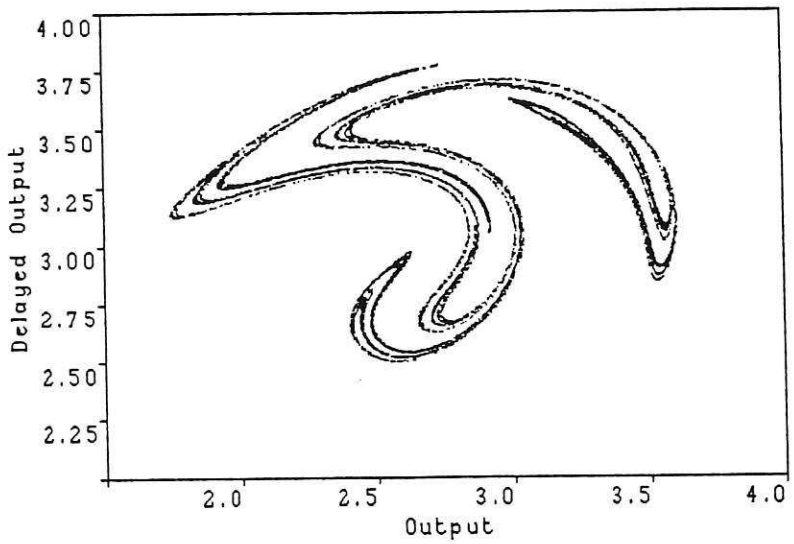

Figure 5b

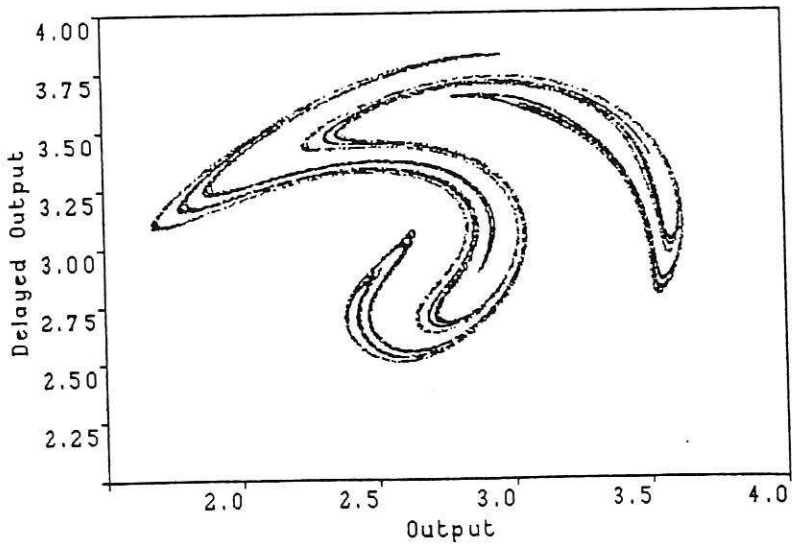

Figure 5c

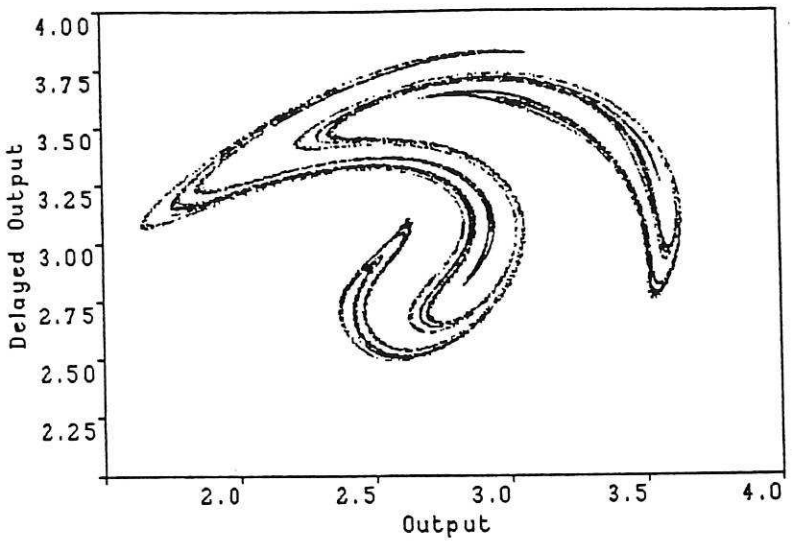

FIGURE 5d

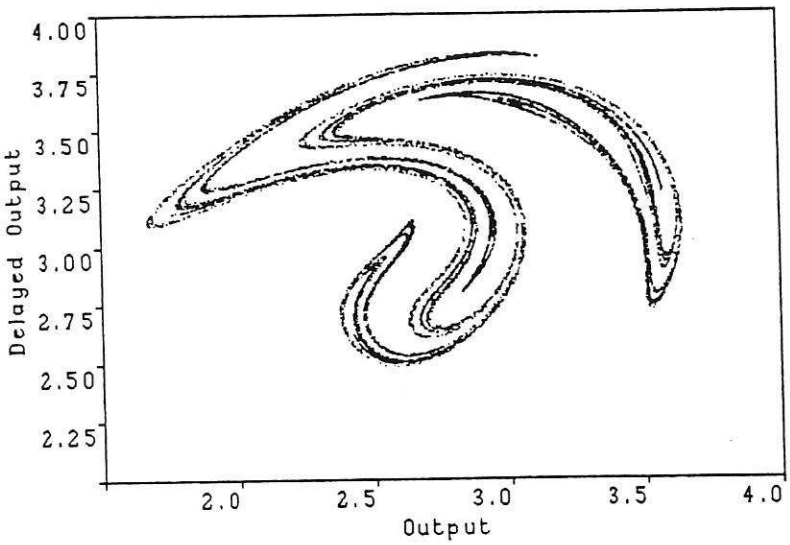

Figure 5e

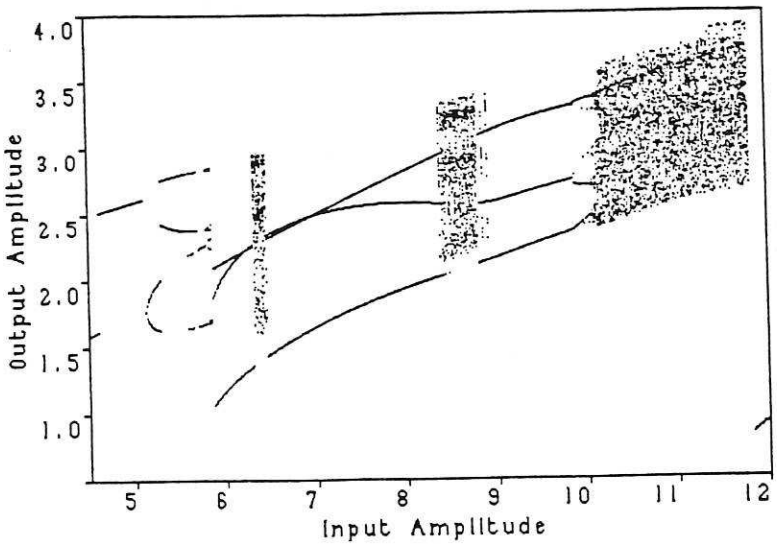

FIGURE 6a

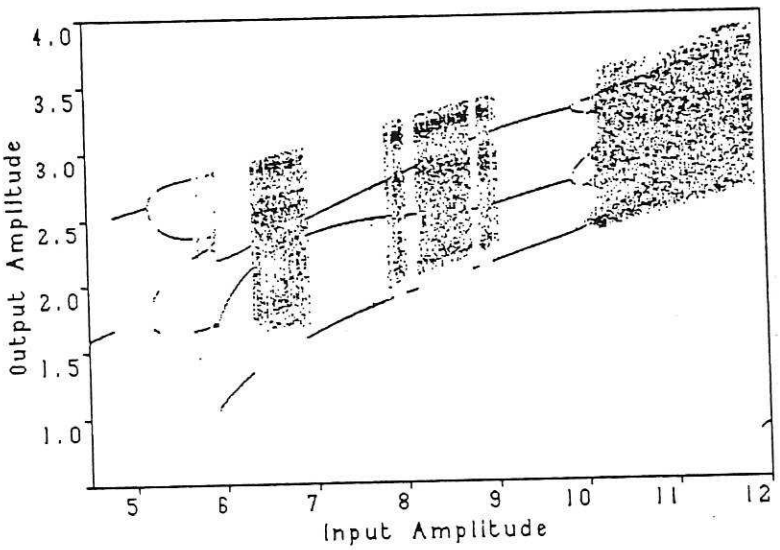

FIGURE 6b

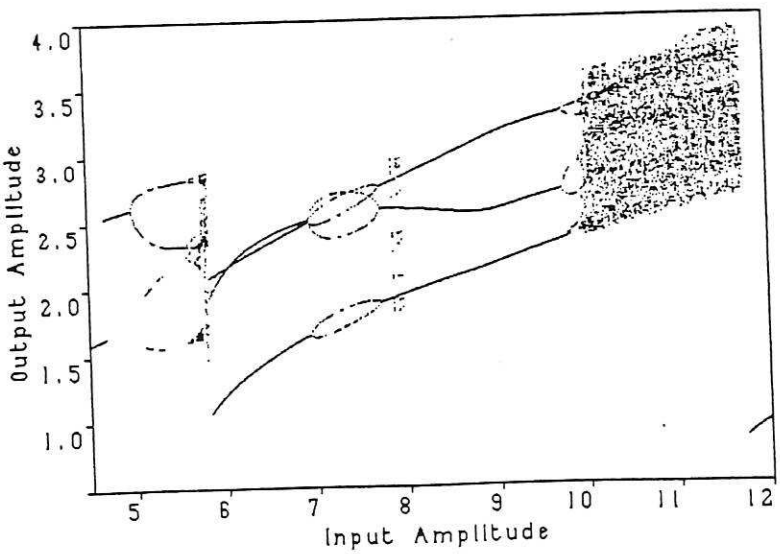

FIGURE 6c

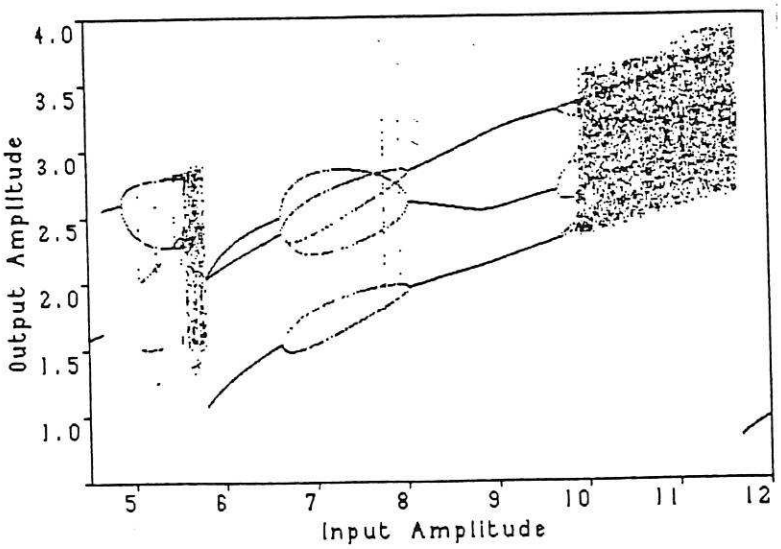

FIGURE 6d

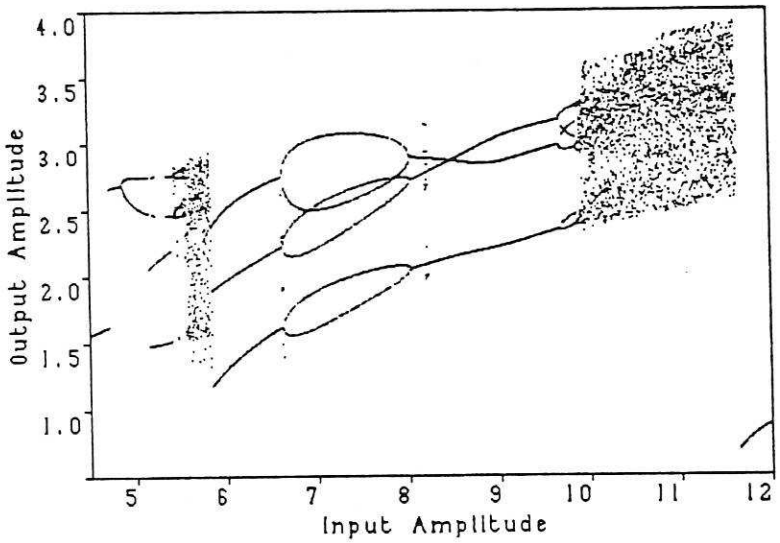

FIGURE 6e

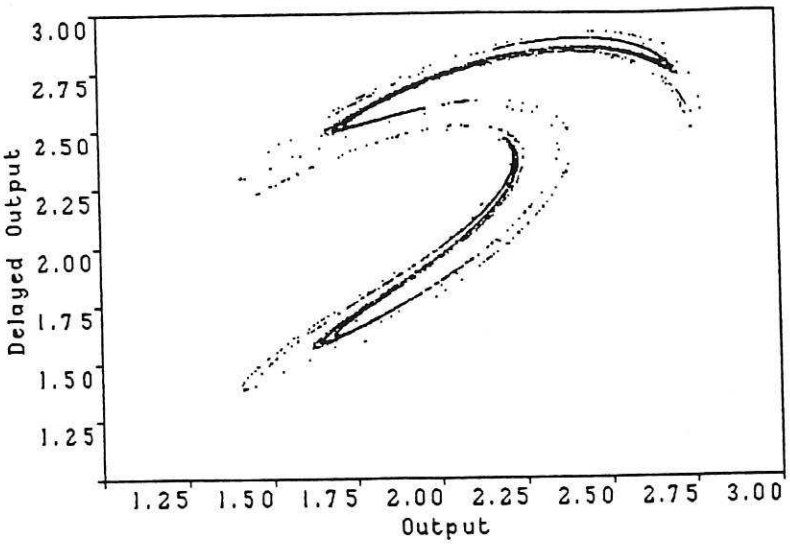

FIGURE 7a

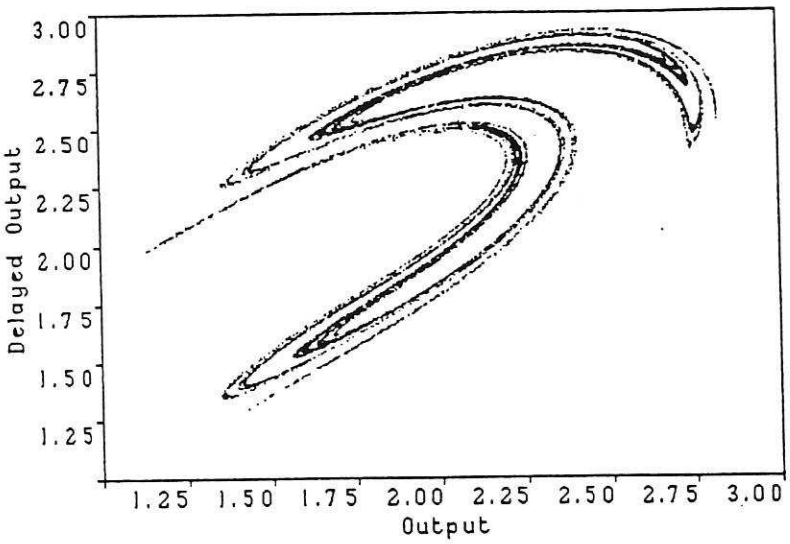

FIGURE 7b

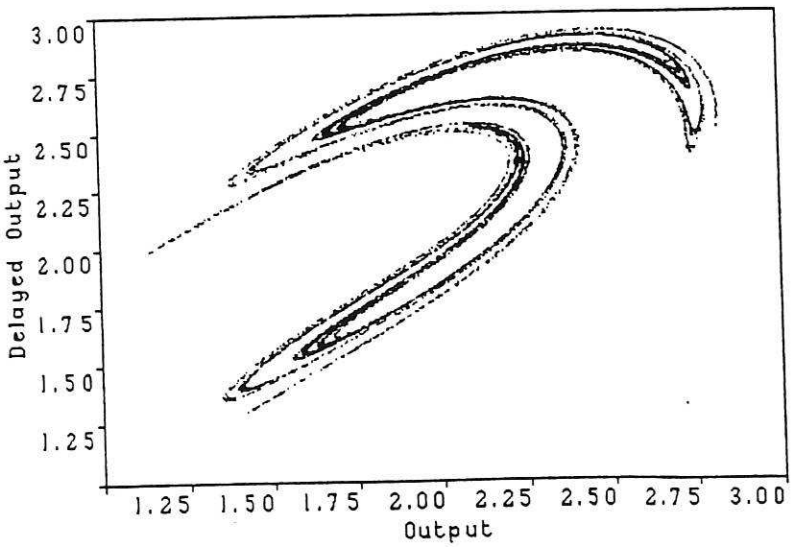

FIGURE 7c